



CoFe Nanoparticles in Carbon Nanofibers as an Electrode for Ultra-Stable Supercapacitor

U. Kurtan¹ · U. Sahinturk² · H. Aydın^{3,4} · D. Dursun^{3,5} · A. Baykal⁶

Received: 28 January 2020 / Accepted: 27 March 2020 / Published online: 1 April 2020
© Springer Science+Business Media, LLC, part of Springer Nature 2020

Abstract

In this paper, we proposed the synthesis of CoFe nanoparticles (NPs) which have been deposited on carbon nanofibers (CNFs) with a facile electrospinning route followed by thermal reduction. The performance of obtained CNF supercapacitors are improved from 51 to 190 F/g (247 mF/cm²) at 0.5 A/g with the combination of CoFe NPs and graphitized carbon layers. The device possessed an energy and power density of 6.6 Wh/kg and 125 W/kg, respectively. Furthermore, the capacitance retention can still maintain about 96.6% after 10,000 cycle test and it is worth noting that the cycling stability is ultrahigh. This research proves that bimetallic nanoparticles embedded in CNFs can elucidate new insights into the development new nanofiber electrode materials for the next generation of symmetric supercapacitors.

Keywords Electrospinning · Carbon nanofibers · CoFe nanoparticles · Energy storage · Supercapacitors

1 Introduction

As next-generation novel energy sources, supercapacitors (SCs) are receiving growing attention because of their ultra high charge rate and excellent power density compared to

the traditional capacitors [1–3]. With respect to their charge storage principle, they are categorized into two groups based on the electrode material: electric double layer capacitors (EDLCs) and pseudocapacitors (PCs). In EDLC, capacitance is generated from the charge separation at the interfaces between a porous electrode material and an electrolyte without any electron transfer whereas PCs utilize faradic reactions. Carbonaceous materials are regarded as typical EDLC materials while metal oxides and conducting polymers are typical pseudocapacitive materials that have relatively good capacitance [4–6]. Among carbonaceous materials, carbon nanofibers (CNFs) especially have received more and more interest from researchers since they have excellent characteristics such as high porosity and good chemical durability but challenges still remain because of the low capacitance of CNFs thus the electrochemical properties of CNFs need to be improved. CNFs can be fabricated by numerous methods including chemical vapor deposition or laser process but these techniques can be sometimes difficult and high cost. Alternatively, the electrospinning technique is the most used method since it is easy and economic for the preparation of nanofibers [7]. Metal oxides including RuO₂, MnO_x, and Co₃O₄ combining with carbon materials have received more attention by scientists for electrochemical capacitors [8, 9]. Because the development of newly electrode materials with high capacitance is strongly desirable. On the other hand, various papers have been reported the combination of CoFe

Electronic supplementary material The online version of this article (<https://doi.org/10.1007/s10904-020-01524-7>) contains supplementary material, which is available to authorized users.

✉ U. Kurtan
umran.kurtan@istanbul.edu.tr

¹ Department of Materials and Materials Processing Technology, Vocational School of Technical Sciences, Istanbul University-Cerrahpasa, 34500 Istanbul, Turkey

² Department of Mechanical and Metal Technology, Vocational School of Technical Sciences, Istanbul University-Cerrahpasa, 34500 Istanbul, Turkey

³ Bionanotronic Medical Engineering Co., Inc., 34164 Istanbul, Turkey

⁴ Department of Chemistry, Istanbul University-Cerrahpasa, 34320 Istanbul, Turkey

⁵ Department of Chemistry, Yıldız Technical University, 34210 Istanbul, Turkey

⁶ Department of Nanomedicine Research, Institute for Research and Medical Consultations (IRMC), Imam Abdulrahman Bin Faisal University, P.O. Box 1982, Dammam 31441, Saudi Arabia

nanoparticles with carbon materials for different applications. For instances, hierarchical CoFe-carbon nanosheets using templates by Li et al. and it exhibited an excellent electrocatalytic performance [10]. In other study, various bimetallic NPs embedded in CNFs were fabricated and tested for glucose detection [11]. Yang et al. fabricated CoFe-CNFs and the rapid and sensitive sensing has been achieved [12]. In addition, Cai et al. prepared CoFe alloy NPs impregnated with the carbon nanotubes. When they used for a Zn-air battery application, a high power density of 150 mW cm^{-2} was found [13]. Core-shell CoFe@C particles were encapsulated in polydopamine-derived carbon nanocages by Wang et al. and they found that the obtained sample displayed superior microwave absorption performance [14]. These results indicated that synthesis of CoFe NPs combination with carbon could greatly change the properties of CNFs by the introduction of electro-active materials. Hence, inspired by these studies, we attempted to the synthesis of CoFe NPs in the CNF with a simple electrospun followed by calcination for supercapacitor application. To the best of our knowledge, CoFe NPs combined with CNF has not been reported for the supercapacitor applications in the existing literature. The CoFe@CNF electrode material was synthesized and characterized and supercapacitor application of CoFe@CNF was described for the first time here and it exhibited an effective capacitive behaviour and ultra-high cycling stability.

2 Experimental

2.1 Chemicals

Polyacrylonitrile (PAN, $M_w = 150,000 \text{ g/mol}$) was obtained from Sigma-Aldrich. Dimethylformamide (DMF), cobalt(II) acetylacetonate ($\text{Co}(\text{acac})_2$) and iron nitrate hexahydrate ($\text{Fe}(\text{NO}_3)_3 \cdot 9\text{H}_2\text{O}$) were obtained from Merck and used as received.

2.2 Fabrication of CoFe@CNF Papers

All nanofibers were fabricated with our home-made electrospinning system followed by stabilization and carbonization. The concentration of PAN was adjusted as 8 wt% and the total amount of salt with respect to PAN was as 9.4 wt%. Firstly, 0.8 g of PAN was dissolved in 9.2 g of DMF for 2 h at $80 \text{ }^\circ\text{C}$ and an appropriate amount of salts was added slowly into the solution. It was stirred until a viscous solution was formed. Then, the precursor solution was electrospun. The needle was held at 17 kV with a high power supply. The syringe pump was at the speed of 0.75 ml/h

and a distance of 20 cm between the needle and metal collector was adjusted. The CNFs were collected approximately 5 h later and dried at $60 \text{ }^\circ\text{C}$ in vacuum. The dried fibers were further annealed in air at $280 \text{ }^\circ\text{C}$ ($5 \text{ }^\circ\text{C/min}$) for 2.5 h and carbonized up to $800 \text{ }^\circ\text{C}$ ($2 \text{ }^\circ\text{C/min}$) in N_2 for 2 h. For comparative study, pure CNFs were also prepared without any metallic salts.

2.3 Characterization

In order to confirm the chemical bonds broken and formed in the CNFs, the samples were subjected to a Fourier Transformed-IR spectroscopy analysis with a Bruker instrument scanned from 4000 to 400 cm^{-1} . To identify the crystalline structure of CNFs, Rigaku D/Max—IIIC was used. The surface morphology of the nanofibers was characterized by scanning electron microscope (JEOL JSM-7001F SEM). Brunauer Emmett Teller (BET, Quantachrome—Quadrasorb Evo 4) analyser was utilized to find the specific surface area and the total pore volume was estimated based on the Density Functional Theory (DFT).

2.4 Electrochemical Studies

The electrochemical characterizations of CNFs have been analyzed by cycle voltammetry (CV) and electrochemical impedance spectroscopy (EIS) on a Gamry Interface 1010B potentiostat-galvanostat-ZRA. Galvanostatic charge-discharge measurements (GCD) were done from 0.5 to 3 A/g

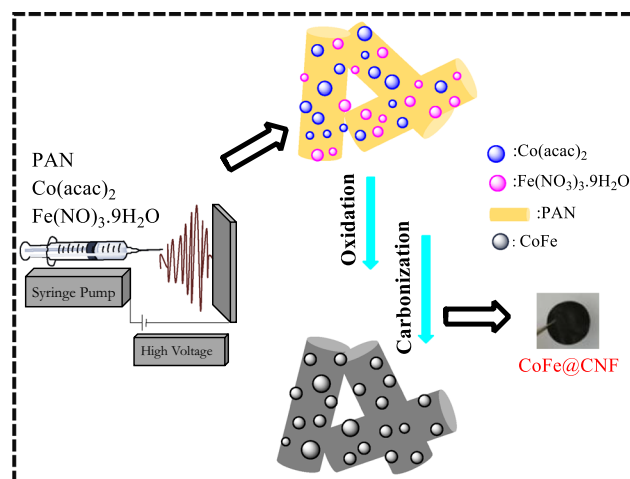


Fig. 1 Schematic diagram for the fabrication of CoFe@CNFs

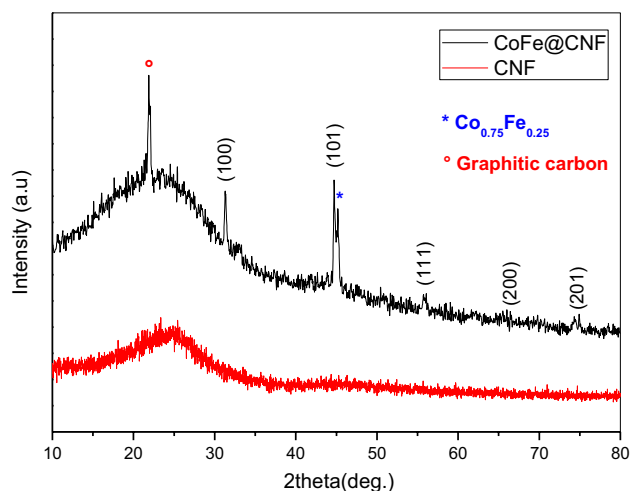


Fig. 2 XRD powder patterns of CNF and CoFe@CNFs samples

current densities by using a 8 channel MTI battery analyzer (10 mA, up to 5 V). To realize commercial application, pure CNF and CoFe@CNF papers were directly used by cutting into self-supported electrodes and the supercapacitors were tested with a Swagelok-type cell in two-electrode system. The electrolyte solution was 1 M H_2SO_4 while the separator was whatman glass fiber (GF/D). Neither any binder nor conductive agents were needed (Fig. 1).

3 Results and Discussion

3.1 XRD Study

The XRD powder patterns of CNF and CoFe@CNF samples have been depicted in Fig. 2. As shown in Fig. 2, the diffraction peak located at $2\theta = 22^\circ$ was observed corresponding to the crystalline plane (002) plane of graphitic carbon [15, 16]. The peaks located at $2\theta = 31.4^\circ$, 44.9° , 56° , 65.4° and 80° correspond to the (100), (101), (111), (200) and (201) crystal planes of CoFe alloy (JCPDS file no. 96-900-4230) which are compatible with the other studies [11, 15–17]. It also proves that the metal species in CoFe@CNF are also present at $2\theta = 45.1^\circ$ as $\text{Co}_{0.75}\text{Fe}_{0.25}$ phase (JCPDS file no. 96-152-4168). As a result, X-ray diffraction patterns confirmed the existence of well crystallized CoFe NPs with a cubic structure and improved the graphitization degree of CNFs by the addition metallic salts [18–20].

3.2 Spectral Analysis

To investigate the chemical structures of as-synthesized samples, FT-IR was conducted. The FT-IR spectra of as-spun

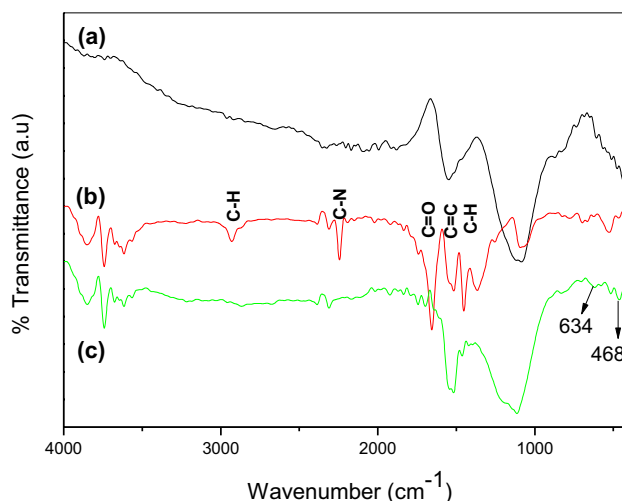


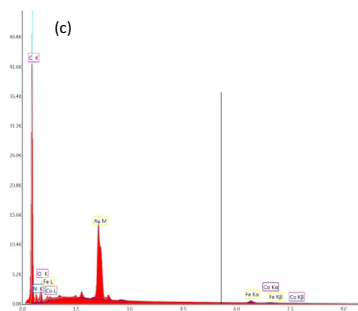
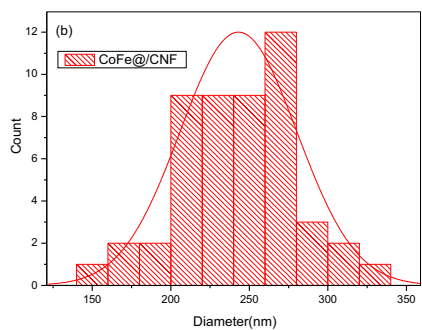
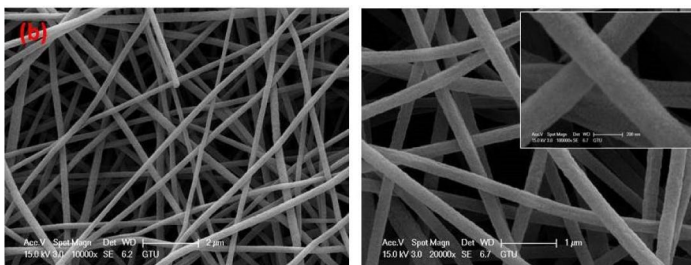
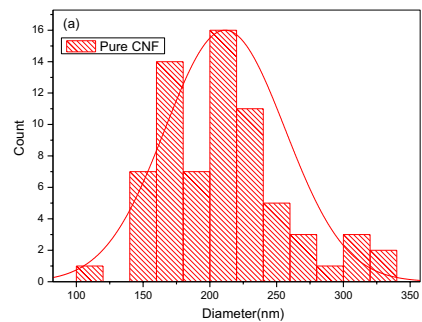
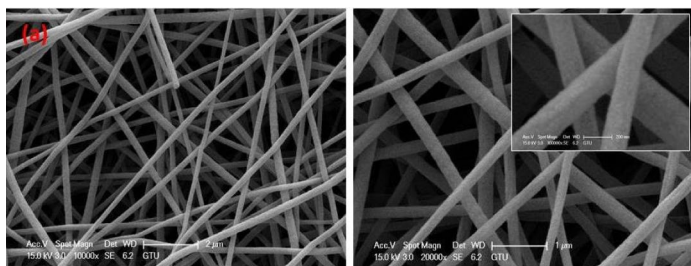
Fig. 3 FT-IR plots of (a) CNF, (b) as-spun precursor nanofibers and (c) CoFe@CNF

precursor nanofibers, CNF, and CoFe@CNF samples are shown in Fig. 3a–c. Figure 3b represents multiple peaks at 2242 , 1653 and 1450 cm^{-1} correspond to PAN polymer functional groups of $-\text{C}\equiv\text{N}$, $\text{C}=\text{O}$, and CH_2 , respectively [16, 21]. Because of the cyclization of nitrile groups in the stabilization process, CNFs displayed the disappearance of various functional groups and produced graphitized structure during carbonization. Two common peaks of CNFs at ~ 1100 and 1556 cm^{-1} were seen which are ascribed to the stretching modes of $\text{C}-\text{C}$ and $\text{C}=\text{C}$ bonds, respectively as seen in Fig. 3a [22, 23]. The peaks at 3500 cm^{-1} can arise from $\text{O}-\text{H}$ stretching and weak bands appearing in spectrum were attributed to the stretching bands of metallic interactions in CNF at about 634 and 468 cm^{-1} in Fig. 3c. Additionally, as a comparison, the spectrum of the CoFe@CNF did not show any peak belongs to NO_3^- , indicating that PAN nanofiber was completely carbonized (Fig. 3c).

3.3 Surface Morphology

The SEM images and particle size distribution diagrams of the electrospun pure CNF and CoFe@CNF samples are presented in Fig. 4. The all products showed uniform bead-free nanofibers and high aspect ratios with a netlike structure. Pure CNFs have a diameter size of $211 \pm 45\text{ nm}$ whereas an average size diameter of $243 \pm 37\text{ nm}$ was seen for CoFe@CNFs. It is clear that encapsulating CoFe alloy nanoparticles into CNFs caused an increase diameter of nanofibers. Our assumption is that while CoFe nanoparticles are formed with the leaving empty space behind in the CNF matrix resulting in increase of diameter of fibers which is in consistence

Fig. 4 Representative SEM images of the obtained **a** CNF and **b** CoFe@CNFs with various magnifications. **c** EDX spectrum of CoFe@CNFs



with what has been seen in literature [24]. Further, the particle size distribution charts confirm that the diameters of the CoFe@CNFs changed uniformly compared to the pure CNFs resulting more regular nanofiber formation. As a result, all fibers are interconnected with each other which can need a continuous pathway for electrolyte diffusion during electrochemical process. The EDX spectrum of CoFe@CNFs is shown in Fig. 4c. The EDX spectrum of CoFe@CNFs shows the prominent peaks from Co, Fe, C, N and O elements which directly confirm the formation of CoFe@CNFs. After stabilization and carbonization process the CoFe@CNFs includes totally 2,38 wt% Co and Fe elements.

3.4 Electrochemical Studies

The CV measurements were done at different scan rates of 1–100 mV/s (Fig. 5a). The electrodes of pure CNFs in supercapacitors did not have any redox peaks, which is a typical

feature of double layer. It showed a good linearity even at high scan rate of 100 mV/s suggesting a good rate capability of the device [25]. In the CV curve of CoFe@CNFs (35 μm electrode thickness), rectangular-like shape was observed, and the CV curves reserved their shape at all scan rates indicating rapid and efficient charge transfer (Fig. 5b). The galvanostatic charge–discharge (GCD) is an accurate technique to investigate the electrochemical performance of SCs. In two electrode symmetric cell configuration, the specific capacitance for a single electrode (C_{sp}) was calculated from galvanostatic charge–discharge curves from Eq. 1 [26–28]:

$$C_{\text{sp}}(\text{F/g}) = (2 \times I \times \Delta t) / (m \times \Delta V) \quad (1)$$

where $I(\text{A})$ is the discharge current, $t(\text{s})$ is the discharge time, $m(\text{g})$ is the mass of single active electrode material and $V(\text{V})$ is the potential windows excluding internal resistance (IR) drop. The energy (E) and power (P) densities are also

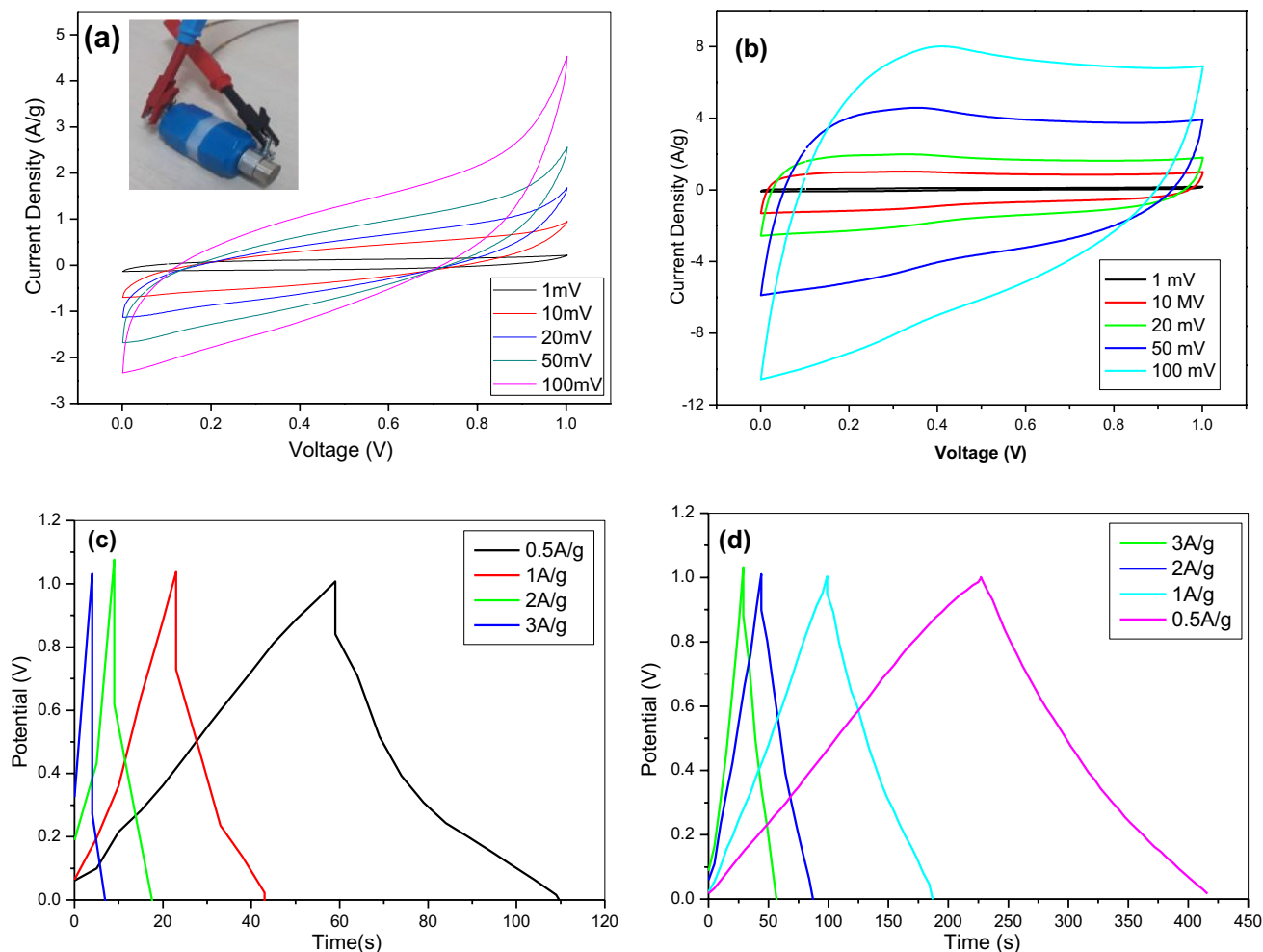


Fig. 5 a, b CV curves of pure CNF and CoFe@CNF and c, d Galvanostatic charge–discharge curves of pure CNF and CoFe@CNF under different current densities. (The inset shows the typical supercapacitor cell)

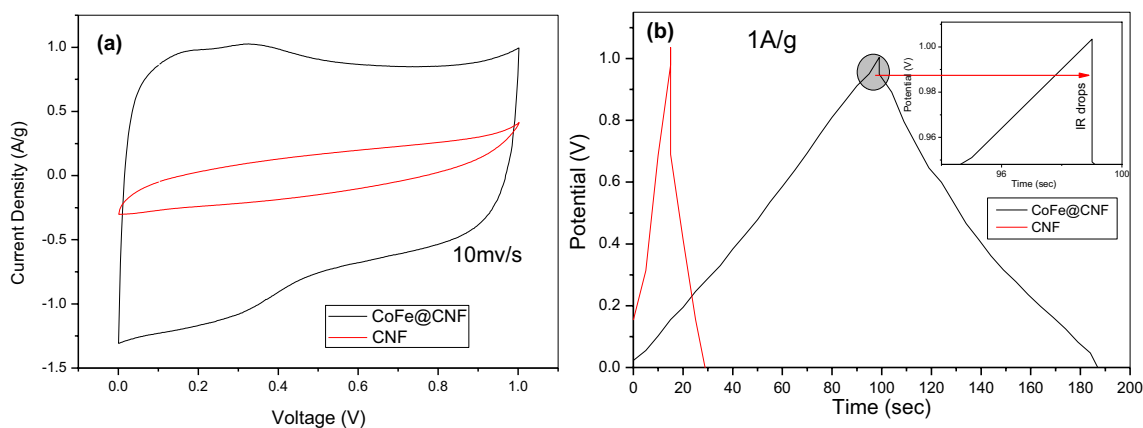


Fig. 6 **a** CV curves and **b** Galvanostatic charge/discharge curves of pure CNF and CoFe@CNF based supercapacitors

very critical performance metrics of supercapacitors, which are found from their GCD curve with Eqs. 2 and 3 [29–31]:

$$E(\text{Wh/kg}) = 1/8 \times C_{\text{sp}}(-V)^2 / (3.6) \quad (2)$$

$$P(\text{W/kg}) = (3600 \times E) / -t \quad (3)$$

Figure 5c, d show GCD curves of CNF and CoFe@CNF based supercapacitor (SC) in the range of 0.5–3 A/g, respectively. The specific capacitance of the pure CNF electrode is 51 F/g while CoFe@CNF based SC was 190 F/g at 0.5 A/g which was 3.8 times higher specific capacitance. Even at a high discharge current density of 3 A/g, it had a specific capacitance of 168 F/g which is ascribed to the mesoporous structure. Additionally, the device exhibited an energy density of 6.6 Wh/kg with a power density of

125 W/kg at 0.5 A/g for CoFe@CNF based electrodes calculated from the Eqs. 2 and 3. Besides, the device is utilized at 3 A/g, its power density increased to 746 W/kg with 5.8 Wh/kg remaining energy density, which are higher than those reported in the literature [32–36]. The surface area and the porosity of CoFe@CNF samples were analyzed with Brunauer Emmett Teller (BET) by the N_2 adsorption–desorption isotherms at 77 K and compared with pure CNF (Figs. S1, S2). The obtained results showed that the surface area (184 m^2/g) and V_t , total volume, (0.28 cm^3/g) of the CoFe@CNF is greater than pure CNF. We could infer that the CoFe alloy NPs created suitable pore structure on the surface of CNFs during stabilization and carbonization from these results. Thus, the existence of enough mesopores in the CNF electrode will ensure not only the enough free space for charge–discharge but also rapid transport for ions and

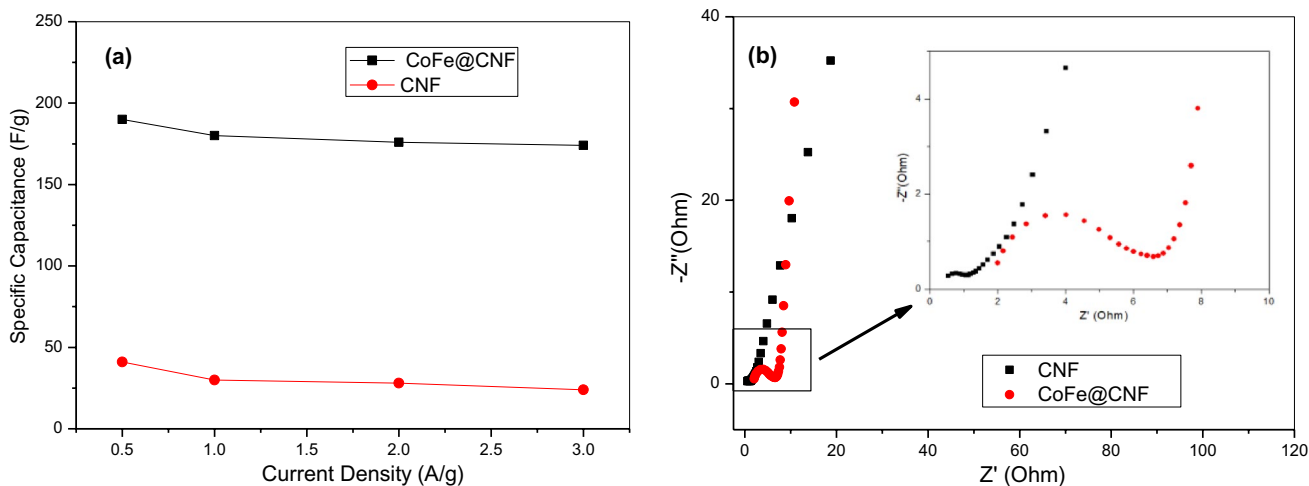


Fig. 7 **a** The specific capacitances calculated from GCD curves at 0.5–3 A/g and **b** Nyquist impedance plots of pure CNF and CoFe@CNF based supercapacitors

electrons [37–41]. The improved specific surface area along with mesoporous nature makes the CoFe@CNF hybrid nanoarchitectures more ideal materials for supercapacitors application.

As it can be seen from Fig. 6a, the CV rectangular area of the chemically deposited CoFe nanoparticles in CNF was much higher than pure CNFs, meaning a promotion of electrochemical performance. This is attributed to the utilization of the CoFe NPs for easier ionic charge transport [15, 42–44]. Figure 6b demonstrates the GCD curves of CNF and CoFe@CNF based supercapacitor device at 1 A/g. Both GCD curves were symmetric triangular shapes but a relatively big IR (internal resistance) was found for pure CNF. On the other hand, a small IR drop (inset of Fig. 6b) was

seen for the corresponding curve of CoFe@CNF owing to an efficient transfer of the electrolyte to the electrode surface and an enhanced electrical conductivity.

Figure 7a represents the variation of specific capacitances of pure CNF and CoFe@CNF electrodes at 0.5–3 A/g calculated according to the Eq. 1. The C_{sp} decreased with the increasing current density for both pure CNF and CoFe@CNF based supercapacitors. This can be explained by two reasons. First, the longer interaction time between electrode and electrolyte ions at low current density helps to store a large amount of charge in the electrode, allowing a higher specific capacitance. The other is that the required time is limited between electrode and electrolyte at high current density thus a lower specific capacitance is obtained. The

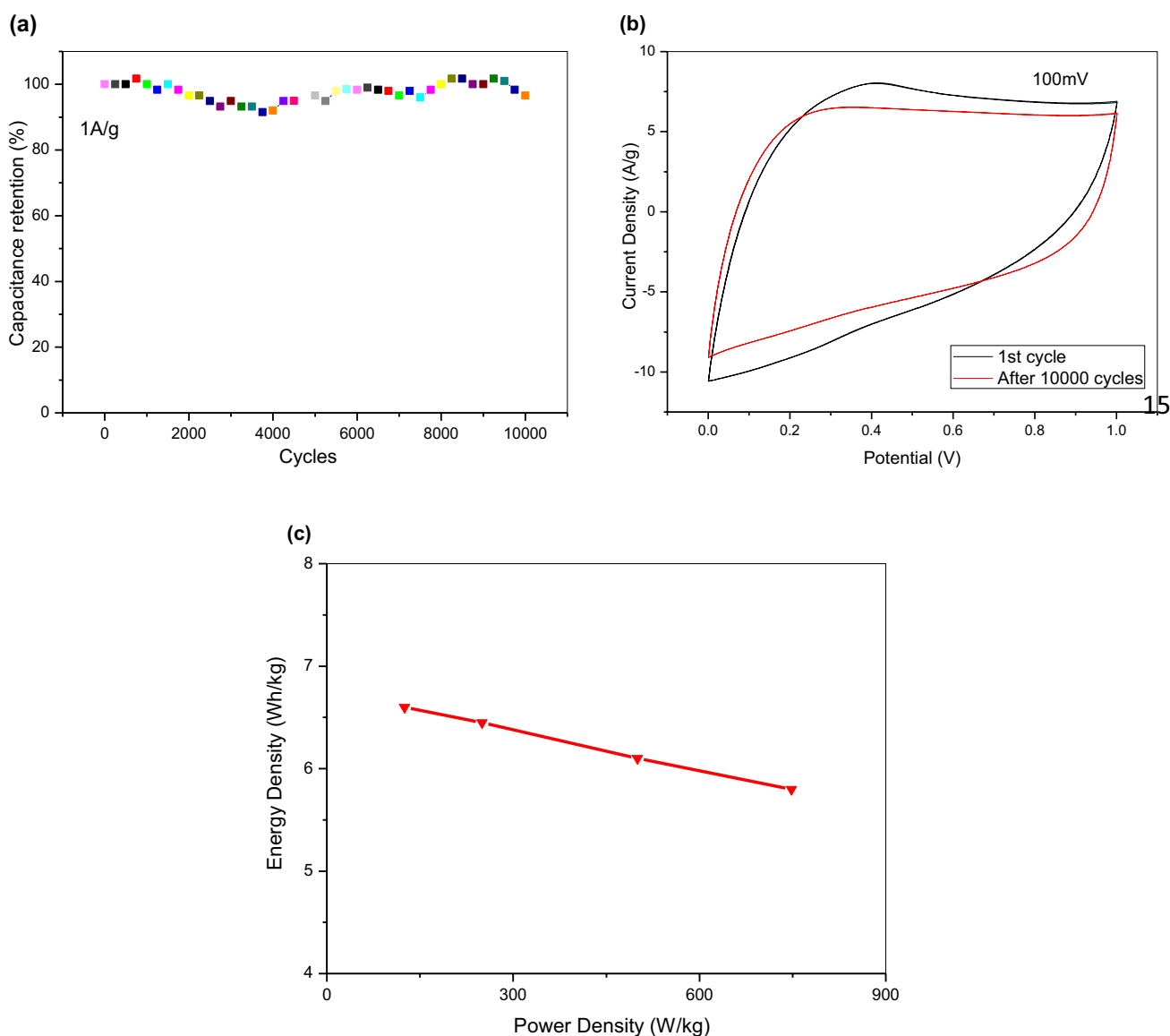


Fig. 8 **a** Cycling stability, **b** Electrochemical stability of CoFe@CNF based supercapacitor at 1st and 10000th cycles and **c** Ragone plot of the fabricated device

impedance Nyquist plots of the pure CNF and CoFe@CNF based supercapacitors were presented in Fig. 7b. The higher charge transfer resistance was observed which is attributed to the enhanced pseudocapacitive behaviour of the CoFe and a similar behaviour was also found in the literature [32, 45, 46].

Figure 8a presents the cycling stability test of the CoFe@CNF electrodes and it showed a good rate performance with 96.6% retention even after 10,000 cycles at 1 A/g. Accordingly, CoFe nanoparticles in CNF provided a good ion mobility resulting a stable structure of the carbon matrix during cycling process. The CV at 1st and after 10,000 cycling stages is presented in Fig. 8b. The reduction in specific capacitance might be due to loss of electrode material during cycling and such a low degradation of 3.4% demonstrates the good electrochemical stability of electrode material. Figure 8c represents CoFe nanoparticles doped CNF based supercapacitors possessed an energy density between ~5.8 and ~6.6 Wh/kg, which was higher than that in previous reports [47–49].

4 Conclusion

In summary, we fabricated bimetallic CoFe nanoparticles with a in-situ process on a carbon network and the resulting CoFe@CNFs electrode material can be used as a self-standing and binder-free electrode for supercapacitors. The assembled symmetric supercapacitor cell delivered the higher capacitance of 190 F/g at 0.5 A/g, good rate ability (174 F/g at 3 A/g) and an excellent cycling stability (only 3.4% loss in capacitance after 10,000 cycles) compared to the pure CNF supercapacitor. Besides, the fabricated CoFe@CNFs supercapacitor delivered an energy and power density of 6.6 Wh/kg and 125 W/kg at 0.5 A/g, respectively. In addition, a energy density of 5.8 Wh/kg is retained when the power density increases to 746 W/kg. Better supercapacitor performance could be explained by the synergistic effect of bimetallic NPs and carbon material and high surface area. Therefore, in-situ preparation of CoFe NPs in CNF can elucidate for the development of new electrode materials for various energy devices.

Acknowledgements This work was supported by the Scientific and Technological Research Council of Turkey TUBITAK (TEY-DEB-1509) International Industrial R&D Project and EU (ERANET-INCOMERA) programme under the Project Number 9160035.

References

1. Y. Liu, J. Zhou, L. Chen, P. Zhang, W. Fu, H. Zhao, Y. Ma, X. Pan, Z. Zhang, W. Han, Highly flexible freestanding porous carbon nanofibers for electrodes materials of high-performance all-carbon supercapacitors. *ACS Appl. Mater. Interfaces*. **7**, 23515–23520 (2015)
2. H.S. Huang, K.H. Chang, N. Suzuki, Y. Yamauchi, C.C. Hu, K.C.W. Wu, Evaporation-induced coating of hydrous ruthenium oxide on mesoporous silica nanoparticles to develop high-performance supercapacitors. *Small* **9**, 2520–2526 (2013)
3. B. Ashourirad, M. Demir, R.A. Smith, R.B. Gupta, H.M. El-Kaderi, Rapid transformation of heterocyclic building blocks into nanoporous carbons for high-performance supercapacitors. *RSC Adv*. **8**, 12300–12309 (2018)
4. C. Fu, A. Mahadevegowda, P.S. Grant, Fe₃O₄/carbon nanofibres with necklace architecture for enhanced electrochemical energy storage. *J. Mater. Chem. A* **3**, 14245–14253 (2015)
5. L.L. Zhang, R. Zhou, X. Zhao, Graphene-based materials as supercapacitor electrodes. *J. Mater. Chem.* **20**, 5983–5992 (2010)
6. M. Demir, B. Ashourirad, J.H. Mugumya, S.K. Saraswat, H.M. El-Kaderi, R.B. Gupta, Nitrogen and oxygen dual-doped porous carbons prepared from pea protein as electrode materials for high performance supercapacitors. *Int. J. Hydrogen Energy* **43**, 18549–18558 (2018)
7. U. Kurtan, D. Dursun, H. Aydın, M.S. Toprak, A. Baykal, A. Bozkurt, Influence of calcination rate on morphologies and magnetic properties of MnFe₂O₄ nanofibers. *Ceram. Int.* **42**, 18189–18195 (2016)
8. Y.A. Kim, B.-H. Kim, Capacitive properties of hierarchically structured carbon nanofiber/graphene/MnO₂ hybrid electrode with nitrogen and oxygen heteroatoms. *Carbon* **107**, 783–791 (2016)
9. X. Yuan, X. Yan, C. Zhou, J. Wang, D. Wang, H. Jiang, Y. Zhu, X. Tao, X. Cheng, Decorating carbon nanosheets with copper oxide nanoparticles for boosting the electrochemical performance of symmetric coin cell supercapacitor with different electrolytes. *Ceram. Int.* **46**, 435–443 (2020)
10. S. Li, C. Cheng, X. Zhao, J. Schmidt, A. Thomas, Active salt/silica-templated 2D mesoporous FeCo-N_x-carbon as bifunctional oxygen electrodes for zinc-air batteries. *Angew. Chem. Int. Ed.* **57**, 1856–1862 (2018)
11. M. Li, L. Liu, Y. Xiong, X. Liu, A. Nsabimana, X. Bo, L. Guo, Bimetallic MCo (M=Cu, Fe, Ni, and Mn) nanoparticles doped-carbon nanofibers synthesized by electrospinning for nonenzymatic glucose detection. *Sens. Actuators B* **207**, 614–622 (2015)
12. Z. Yang, Y. Zhu, G. Nie, M. Li, C. Wang, X. Lu, FeCo nanoparticles-embedded carbon nanofibers as robust peroxidase mimics for sensitive colorimetric detection of L-cysteine. *Dalton Trans.* **46**, 8942–8949 (2017)
13. P. Cai, Y. Hong, S. Ci, Z. Wen, In situ integration of CoFe alloy nanoparticles with nitrogen-doped carbon nanotubes as advanced bifunctional cathode catalysts for Zn-air batteries. *Nanoscale* **8**, 20048–20055 (2016)
14. F. Wang, N. Wang, X. Han, D. Liu, Y. Wang, L. Cui, P. Xu, Y. Du, Core-shell FeCo@ carbon nanoparticles encapsulated in polydopamine-derived carbon nanocages for efficient microwave absorption. *Carbon* **145**, 701–711 (2019)
15. X. Liu, L. Wang, P. Yu, C. Tian, F. Sun, J. Ma, W. Li, H. Fu, A stable bifunctional catalyst for rechargeable zinc-air batteries: iron-cobalt nanoparticles embedded in a nitrogen-doped 3D carbon matrix. *Angew. Chem.* **130**, 16398–16402 (2018)
16. H. Wang, W. Wang, H. Wang, X. Jin, H. Niu, H. Wang, H. Zhou, T. Lin, High performance supercapacitor electrode materials from electrospun carbon nanofibers in situ activated by high decomposition temperature polymer. *ACS Appl. Energy Mater.* **1**, 431–439 (2018)
17. B. Jeong, D. Shin, J.K. Lee, D.H. Kim, Y.D. Kim, J. Lee, The influence of a fibrous carbon envelope on the formation of CoFe

- nanoparticles for durable electrocatalytic oxygen evolution. *Phys. Chem. Chem. Phys.* **16**, 13807–13813 (2014)
18. N. Cai, M. Chen, M. Liu, J. Wang, L. Shen, J. Wang, X. Feng, F. Yu, Meso-microporous carbon nanofibers with in-situ embedded Co nanoparticles for catalytic oxidization of azo dyes. *J. Mol. Liq.* **289**, 111060 (2019)
 19. K. He, J. Zai, X. Liu, Y. Zhu, A. Iqbal, T. TadesseTsega, Y. Zhang, N. Ali, X. Qian, One-step construction of multi-doped nanoporous carbon-based nanoarchitecture as an advanced bifunctional oxygen electrode for Zn-Air batteries. *Appl. Catal. B* **265**, 118594 (2020)
 20. Y. Zhang, J. Zai, K. He, X. Qian, Fe₃C nanoparticles encapsulated in highly crystalline porous graphite: salt-template synthesis and enhanced electrocatalytic oxygen evolution activity and stability. *Chem. Commun.* **54**, 3158–3161 (2018)
 21. E. Ismar, T. Karazehir, M. Ates, A.S. Sarac, Electrospun carbon nanofiber web electrode: supercapacitor behavior in various electrolytes. *J. Appl. Polym. Sci.* **135**, 45723 (2018)
 22. T. Zhang, D. Huang, Y. Yang, F. Kang, J. Gu, Influence of iron (III) acetylacetonate on structure and electrical conductivity of Fe₃O₄/carbon composite nanofibers. *Polymer* **53**, 6000–6007 (2012)
 23. S. Nilmouring, P. Kidkhunthod, S. Pinitsoontorn, S. Rujirawat, R. Yimnirun, S. Maensiri, Fabrication, structure, and magnetic properties of electrospun carbon/cobalt ferrite (C/CoFe₂O₄) composite nanofibers. *Appl. Phys. A* **119**, 141–154 (2015)
 24. S. Kim, B. Bajaj, C.K. Byun, S.-J. Kwon, H.-I. Joh, K.B. Yi, S. Lee, Preparation of flexible zinc oxide/carbon nanofiber webs for mid-temperature desulfurization. *Appl. Surf. Sci.* **320**, 218–224 (2014)
 25. X. Hao, J. Wang, B. Ding, Z. Chang, Y. Wang, H. Dou, X. Zhang, Nitrogen-doped porous carbon nanospheres from natural sepia ink: easy preparation and extraordinary capacitive performance. *ChemNanoMat* **3**, 895–901 (2017)
 26. L. Qie, W. Chen, H. Xu, X. Xiong, Y. Jiang, F. Zou, X. Hu, Y. Xin, Z. Zhang, Y. Huang, Synthesis of functionalized 3D hierarchical porous carbon for high-performance supercapacitors. *Energy Environ. Sci.* **6**, 2497–2504 (2013)
 27. D. Liu, W. Zhang, H. Lin, Y. Li, H. Lu, Y. Wang, Hierarchical porous carbon based on the self-templating structure of rice husk for high-performance supercapacitors. *RSC Adv.* **5**, 19294–19300 (2015)
 28. B.S. Mao, Z. Wen, Z. Bo, J. Chang, X. Huang, J. Chen, Hierarchical nanohybrids with porous CNT-networks decorated crumpled graphene balls for supercapacitors. *ACS Appl. Mater. Interfaces.* **6**, 9881–9889 (2014)
 29. J. Li, G. Zhang, C. Fu, L. Deng, R. Sun, C.-P. Wong, Facile preparation of nitrogen/sulfur co-doped and hierarchical porous graphene hydrogel for high-performance electrochemical capacitor. *J. Power Sources* **345**, 146–155 (2017)
 30. H. Wang, H. Yi, X. Chen, X. Wang, Asymmetric supercapacitors based on nano-architected nickel oxide/graphene foam and hierarchical porous nitrogen-doped carbon nanotubes with ultrahigh-rate performance. *J. Mater. Chem. A* **2**, 3223–3230 (2014)
 31. Y.-K. Ahn, B. Kim, J. Ko, D.-J. You, Z. Yin, H. Kim, D. Shin, S. Cho, J. Yoo, Y.S. Kim, All solid state flexible supercapacitors operating at 4 V with a cross-linked polymer–ionic liquid electrolyte. *J. Mater. Chem. A* **4**, 4386–4391 (2016)
 32. X. Liu, M.N. Marlow, S.J. Cooper, B. Song, X. Chen, N.P. Brandon, B. Wu, Flexible all-fiber electrospun supercapacitor. *J. Power Sources* **384**, 264–269 (2018)
 33. Z.-Y. Yu, L.-F. Chen, L.-T. Song, Y.-W. Zhu, H.-X. Ji, S.-H. Yu, Free-standing boron and oxygen co-doped carbon nanofiber films for large volumetric capacitance and high rate capability supercapacitors. *Nano Energy* **15**, 235–243 (2015)
 34. G. He, Y. Song, S. Chen, L. Wang, Porous carbon nanofiber mats from electrospun polyacrylonitrile/polymethylmethacrylate composite nanofibers for supercapacitor electrode materials. *J. Mater. Sci.* **53**, 9721–9730 (2018)
 35. D. Jiménez-Cordero, F. Heras, M.A. Gilarranz, E. Raymundo-Piñero, Grape seed carbons for studying the influence of texture on supercapacitor behaviour in aqueous electrolytes. *Carbon* **71**, 127–138 (2014)
 36. H. Wang, X. Sun, Z. Liu, Z. Lei, Creation of nanopores on graphene planes with MgO template for preparing high-performance supercapacitor electrodes. *Nanoscale* **6**, 6577–6584 (2014)
 37. N. Cai, J. Fu, V. Chan, M. Liu, W. Chen, J. Wang, H. Zeng, F. Yu, MnCo₂O₄@ nitrogen-doped carbon nanofiber composites with meso-microporous structure for high-performance symmetric supercapacitors. *J. Alloy. Compd.* **782**, 251–262 (2019)
 38. N. Cai, J. Fu, H. Zeng, X. Luo, C. Han, F. Yu, Reduced graphene oxide-silver nanoparticles/nitrogen-doped carbon nanofiber composites with meso-microporous structure for high-performance symmetric supercapacitor application. *J. Alloy. Compd.* **742**, 769–779 (2018)
 39. J. Wang, C. Liu, J. Li, R. Luo, X. Hu, X. Sun, J. Shen, W. Han, L. Wang, In-situ incorporation of iron-copper bimetallic particles in electrospun carbon nanofibers as an efficient Fenton catalyst. *Appl. Catal. B* **207**, 316–325 (2017)
 40. G. Wang, J. Zhang, S. Kuang, J. Zhou, W. Xing, S. Zhuo, Nitrogen-doped hierarchical porous carbon as an efficient electrode material for supercapacitors. *Electrochim. Acta* **153**, 273–279 (2015)
 41. M. Demir, S.K. Saraswat, R.B. Gupta, Hierarchical nitrogen-doped porous carbon derived from lecithin for high-performance supercapacitors. *RSC advances* **7**, 42430–42442 (2017)
 42. Y. Lu, K. Fu, S. Zhang, Y. Li, C. Chen, J. Zhu, M. Yanilmaz, M. Dirican, X. Zhang, Centrifugal spinning: A novel approach to fabricate porous carbon fibers as binder-free electrodes for electric double-layer capacitors. *J. Power Sources* **273**, 502–510 (2015)
 43. L.-F. Chen, X.-D. Zhang, H.-W. Liang, M. Kong, Q.-F. Guan, P. Chen, Z.-Y. Wu, S.-H. Yu, Synthesis of nitrogen-doped porous carbon nanofibers as an efficient electrode material for supercapacitors. *ACS Nano* **6**, 7092–7102 (2012)
 44. S.-C. Lin, Y.-T. Lu, Y.-A. Chien, J.-A. Wang, T.-H. You, Y.-S. Wang, C.-W. Lin, C.-C.M. Ma, C.-C. Hu, Asymmetric supercapacitors based on functional electrospun carbon nanofiber/manganese oxide electrodes with high power density and energy density. *J. Power Sources* **362**, 258–269 (2017)
 45. M. Demir, A.A. Farghaly, M.J. Decuir, M.M. Collinson, R.B. Gupta, Supercapacitance and oxygen reduction characteristics of sulfur self-doped micro/mesoporous bio-carbon derived from lignin. *Mater. Chem. Phys.* **216**, 508–516 (2018)
 46. M. Lee, G.-P. Kim, H.D. Song, S. Park, J. Yi, Preparation of energy storage material derived from a used cigarette filter for a supercapacitor electrode. *Nanotechnology* **25**, 345601 (2014)
 47. V. Khomenko, E. Raymundo-Piñero, F. Béguin, A new type of high energy asymmetric capacitor with nanoporous carbon electrodes in aqueous electrolyte. *J. Power Sources* **195**, 4234–4241 (2010)
 48. V. Khomenko, E. Raymundo-Piñero, E. Frackowiak, F. Béguin, High-voltage asymmetric supercapacitors operating in aqueous electrolyte. *Appl. Phys. A* **82**, 567–573 (2006)
 49. L. Deng, Z. Hao, J. Wang, G. Zhu, L. Kang, Z.-H. Liu, Z. Yang, Z. Wang, Preparation and capacitance of graphene/multiwall carbon nanotubes/MnO₂ hybrid material for high-performance asymmetrical electrochemical capacitor. *Electrochim. Acta* **89**, 191–198 (2013)

Publisher's Note Springer Nature remains neutral with regard to jurisdictional claims in published maps and institutional affiliations.